Physiol Genomics 49: 690–702, 2017.
First published September 15, 2017; doi:10.1152/physiolgenomics.00009.2017.

RESEARCH ARTICLE | *Genomics of Metabolic and Tumor/Cancer Traits*

Tissue-, sex-, and age-specific DNA methylation of rat glucocorticoid receptor gene promoter and insulin-like growth factor 2 imprinting control region

Ogechukwu Brenda Agba,[1]* Ludwig Lausser,[2,3]* Klaus Huse,[1] Christoph Bergmeier,[4] Niels Jahn,[1,3,4] Marco Groth,[1] Martin Bens,[1] Arne Sahm,[1] Maria Gall,[4] Otto W. Witte,[4] Hans A. Kestler,[2,3]* Matthias Schwab,[4]* and Matthias Platzer[1]*

[1]*Genome Analysis, Leibniz Institute on Aging - Fritz Lipmann Institute, Jena, Germany;* [2]*Systems Biology of Aging, Leibniz Institute on Aging - Fritz Lipmann Institute, Jena, Germany;* [3]*Institute of Medical Systems Biology, Ulm University, Ulm, Germany; and* [4]*Hans Berger Department of Neurology, Jena University Hospital, Jena, Germany*

Submitted 1 February 2017; accepted in final form 12 September 2017

Agba OB, Lausser L, Huse K, Bergmeier C, Jahn N, Groth M, Bens M, Sahm A, Gall M, Witte OW, Kestler HA, Schwab M, Platzer M. Tissue-, sex-, and age-specific DNA methylation of rat glucocorticoid receptor gene promoter and insulin-like growth factor 2 imprinting control region. *Physiol Genomics* 49: 690–702, 2017. First published September 15, 2017; doi:10.1152/physiolgenomics.00009.2017.—Tissue-, sex-, and age-specific epigenetic modifications such as DNA methylation are largely unknown. Changes in DNA methylation of the glucocorticoid receptor gene (*NR3C1*) and imprinting control region (ICR) of *IGF2* and *H19* genes during the lifespan are particularly interesting since these genes are susceptible to epigenetic modifications by prenatal stress or malnutrition. They are important regulators of development and aging. Methylation changes of *NR3C1* affect glucocorticoid receptor expression, which is associated with stress sensitivity and stress-related diseases predominantly occurring during aging. Methylation changes of *IGF2/H19* affect growth trajectory and nutrient use with risk of metabolic syndrome. Using a locus-specific approach, we characterized DNA methylation patterns of different *Nr3c1* promoters and *Igf2/H19* ICR in seven tissues of rats at 3, 9, and 24 mo of age. We found a complex pattern of locus-, tissue-, sex-, and age-specific DNA methylation. Tissue-specific methylation was most prominent at the shores of the *Nr3c1* CpG island (CGI). Sex-specific differences in methylation peaked at 9 mo. During aging, *Nr3c1* predominantly displayed hypomethylation mainly in females and at shores, whereas hypermethylation occurred within the CGI. *Igf2/H19* ICR exhibited age-related hypomethylation occurring mainly in males. Methylation patterns of *Nr3c1* in the skin correlated with those in the cortex, hippocampus, and hypothalamus. Skin may serve as proxy for methylation changes in central parts of the hypothalamic-pituitary-adrenal axis and hence for vulnerability to stress- and age-associated diseases. Thus, we provide in-depth insight into the complex DNA methylation changes of rat *Nr3c1* and *Igf2/H19* during aging that are tissue and sex specific.

epigenetics; DNA methylation; aging

THE EPIGENETIC STATE of a cell is crucial for the variability of cell function during the entire lifespan (38, 45). DNA methylation in mammals, primarily occurring as 5-methyl C in a CpG dinucleotide context, is one of the basic epigenetic mechanisms (27). CpGs are concentrated in CpG islands (CGIs) enriched at gene promoters. CGIs are hypomethylated in an otherwise CpG-sparse and usually highly methylated genome. The 2 kb of sequence flanking a CGI are defined as "shores" (16, 66). Gene promoters mostly display tissue-specific methylation at their CGI shores (24). Moreover, locus-, tissue-, and sex-specific methylation of genes is known to affect gene transcription (34, 36, 43).

DNA methylation has been described as a well-known hallmark of aging (38). It is known in humans that genome-wide DNA methylation decreases during aging (22), although CpGs located within CGIs become hypermethylated (26). In rats, methyl C content decreases in the brain, heart, skeletal muscle, and liver within 6 mo after birth (23) while, similar to humans, hypermethylation of CGIs is observed at an older age (19). These data imply that for genes having a control function for aging processes such as *NR3C1* coding for the glucocorticoid receptor (13, 18) and the *IGF2/H19* imprinting control region (ICR) (17, 18, 35, 41, 55), detailed characterization of DNA methylation patterns over lifetime is highly desirable.

NR3C1 codes for a ubiquitously expressed receptor that regulates genes involved in stress response, development, metabolism, and immune activity (28, 48, 53, 56, 59, 62). There is evidence that exposure to glucocorticoids in early life can program the function of the hypothalamic-pituitary-adrenal (HPA) axis by epigenetic mechanisms, which in turn has profound effects on functioning and aging of tissues (9, 29, 57, 64). However, studies on *NR3C1* methylation pattern during aging are scanty. Decreased methylation was seen at one analyzed CpG site of the *NR3C1* promoter region in whole blood buffy coats of men during aging (40). Notably, *NR3C1* is a gene with multiple promoters (44, 61, 62) and DNA methylation along these promoters in different tissues during aging is unknown.

Differentially methylated sequence of the ICR regulates the monoallelic expression of *IGF2* and *H19* from opposite parental alleles (60). In the maternal allele, the ICR is unmethylated, while the paternal allele is methylated. Both genes encode molecules controlling fetal growth (4, 14). The Igf2/H19 locus is an important regulator of embryonic development, proliferation of adult pluripotent stem cells, longevity and cancerogenesis (55). Alterations in *IGF2/H19* ICR imprinting are associated with tumors and developmental disorders (31). During aging, loss of imprinting occurs in the mouse and human

* O. B. Agba and L. Lausser contributed equally to this work; H. A. Kestler, M. Schwab, and M. Platzer are joint senior authors of this work.

Address for reprint requests and other correspondence: M. Platzer: Leibniz Inst. on Aging - Fritz Lipmann Inst., Beutenbergstr. 11, 07745 Jena, Germany (e-mail: Matthias.Platzer@leibniz-fli.de).

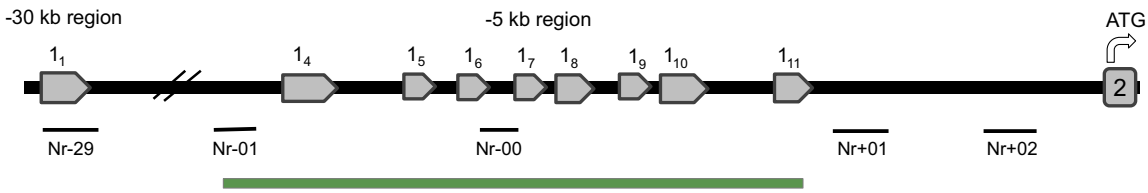

Fig. 1. Promoter structure of rat *Nr3c1*. The location of the alternative first exons (1_1, 1_4, 1_5, 1_6, 1_7, 1_8, 1_9, 1_{10}, 1_{11}; Table 1), the second exon (containing the translation start site) and the analyzed amplicons (Nr−29/−01/−00/+01/+02) are shown. Green bar: CpG island (CGI). Drawings are not to scale. Exon 1_1 and exons 1_{4-11} were annotated with GenBank accession BY121883 and AJ271870, respectively. Exon nomenclature is according to McCormick et al. (44).

prostate associated with increased *Igf2/IGF2* expression (17). In brain, however, *Igf2* mRNA was shown to decline with aging (30).

We carefully chose the *NR3C1* and Igf2/H19 loci as they are prime targets in research on prenatal programming and their methylation changes may explain associations between early environmental influences such as nutrition and stress and the trajectory of brain development and aging (6). To serve as a base for future studies that focus on epigenetically mediated perturbations of development and aging, we set out to analyze *Nr3c1* and *Igf2/H19* ICR methylation changes during the rat lifespan of rats (*Rattus norvegicus*). To determine methylation at single-nucleotide resolution, genomic DNA was treated with bisulfite (BS), amplified, and deeply sequenced (BS Amplicon-seq) for reliable quantification. To study the methylation pattern in the different areas of the *Nr3c1* promoter, we analyzed amplicons at both its proximal (within and at the shores of the CGI) and distal promoter regions. By analyzing six amplicons, seven tissues and three age points, we identified locus-, age-, tissue-, and sex-related changes of *Nr3c1* and *Igf2/H19* methylation. The *NR3C1* promoter structure and the *IGF2/H19* ICR are highly conserved between humans and rats (5, 62). The studied ages of 3, 9, and 24 mo represent adolescence, adulthood, and old age in rats correspond to ~9, 27, and 72 yr in humans (58).

MATERIALS AND METHODS

Animals

All animal procedures were approved by the Animal Welfare Committee of Thuringia, license no. 02-034/12. Wistar rats were obtained from Harlan (Eystrup, Germany) and allowed to acclimate in the animal facility, Institute of Laboratory Animal Science and Welfare at the Jena University Hospital, Jena, Germany, for 8 wk. Animals were maintained in 12 h light cycled room with temperatures between 21 and 27°C and fed with a standard laboratory diet (ssniff, Soest, Germany) and normal drinking water ad libitum. Mating was done pairwise for 24 h at 12 wk of age. Pregnant females were housed and delivered separately. Weaning was done after 23 days, and pups of the same sex were housed together. Litters were culled to a maximum of 10 to ensure standardized nutrition and maternal care of the offspring. We have used offspring of 2–4 litters and 1–5 littermates per age group and sex. Offspring were euthanized at age 3, 9, and 24 mo (eight females and eight males per time point), and seven tissues (Cor, cortex; Hip, hippocampus; Hyp, hypothalamus; Pit, pituitary; Adr, adrenal cortex; Ski, skin; Liv, liver) were sampled. Euthanasia was done by decapitation of rats under deep isoflurane anesthesia. The animals were decapitated when they did not respond to the foot pinch pain test and breathing had ceased. Tissues were shock-frozen in liquid nitrogen and stored at −80°C until DNA isolation. Preparation time was under 5 min. For Pit we used the entire gland and not dissected anterior and posterior parts.

DNA Isolation and Sodium BS Treatment

Generally, 25 mg tissue was homogenized using the Qiagen tissue lyzer at a frequency of 30 Hz for 3 min. DNA isolation was done using the DNeasy Blood & Tissue Kit (Qiagen) and stored at −20°C; ~200 ng DNA was subjected to sodium BS treatment using the Methylation Gold Kit (Zymo Research). PCR was performed immediately after BS treatment.

BS-specific PCR

Five amplicons were selected from the rat *Nr3c1* promoter regions (Fig. 1, Table 1) and one amplicon within the rat *Igf2/H19* ICR. Primers were designed using MethPrimer (33). For reasons of better quality of PCR products and handling, the identity of the six PCR amplicons from each of the seven tissues, mostly nested/seminested PCR was performed. The first PCR was performed with the same pairs of amplicon-specific BS primers in all tissues. Cycling was done using the Bioline PCR mix (BIOLINE) in 25 μl reaction vol. at 94°C for 1 min, 29 cycles at 57°C for 30 s, 72°C for 1 min, 94°C for 30 s, and a final elongation step at 72°C for 5 min; 1:100 dilution of the products was done, and 1 μl of the dilution was used for a second PCR. The second PCR was then performed using tissue-specifically tagged primers (tag: 3 nucleotides at 5′-ends; Table 2). Cycling conditions were the same as in the first PCR except that the number of cycles was reduced to 25. The products were visualized on 1% agarose gels. Table 3 describes the amplicons of the second PCR. Information on primer sequences of the first and second PCR are given in Table 4.

Sequencing

In general Illumina technology was used for library preparation and sequencing. All tissue-specifically tagged amplicons from a single animal were pooled together. For each of these pools an animal-specific indexed sequencing library was prepared using Illumina TruSeq DNA PCR-free library preparation kit following the manu-

Table 1. *Genomic positions of first untranslated exons and CpG island*

	Genomic Positions
Exon 1_1	chr18:32,703,226–32,703,434
Exon 1_4	chr18:32,674,695–32,674,922
Exon 1_5	chr18:32,674,213–32,674,270
Exon 1_6	chr18:32,673,938–32,673,988
Exon 1_7	chr18:32,673,597–32,673,649
Exon 1_8	chr18:32,673,404–32,673,504
Exon 1_9	chr18:32,673,142–32,673,220
Exon 1_{10}	chr18:32,672,880–32,673,080
Exon 1_{11}	chr18:32,672,371–32,672,478
CpG island	chr18:32,672,386–32,675,206

Genomic positions are from Rat Genome version: July 2014 (RGSC 6.0/rn6). GenBank accession BY121883 and AJ271870 were used for the annotation of exon 1_1 and exons 1_{4-11}, respectively. Note that *Nr3c1* is located on the opposite strand of the reference genome sequence.

Table 2. *Tags used to label amplicon sequences according to their tissue origin*

Tag	Tissue
ATG	Cor, cortex
CAT	Hip, hippocampus
CGA	Hyp, hypothalamus
CTC	Pit, pituitary
GAG	Adr, adrenal
GGC	Ski, skin
GTT	Liv, liver

Tags are added at the 5′-end of nested primers.

facturer's protocol with the exception that amplicons (around 500 ng) were directly introduced into end-repair skipping the fragmentation step. The libraries where quantified and quality checked using the Agilent Bioanalyzer 2100 and the Agilent DNA 7500 Kit (Agilent Technologies). Next, libraries were pooled and sequenced using the Illumina MiSeq (2 × 300 cycles, paired-end mode). The read information was extracted by MiSeq Control Software (MCS) v2.4.1.3 or bcl2fastq v2.16 (Illumina). This includes demultiplexing of reads based on the animal-specific Illumina indices and trimming of Illumina adapter sequences.

Data Processing

Sequence data were analyzed for quality control by FastQC. Demultiplexing of reads based on tissue-specific PCR tags was done with an in-house script. Reads were filtered for the expected lengths and the correct primer pair sequences. Only reads derived from molecules that were successfully sequenced in both forward and reverse direction were selected. Chimeras were excluded by filtering the read pairs for identical tags. Sequences have been deposited at the European Nucleotide Archive under the Bioproject accession number PRJEB18949.

Methylation determination was done using SEGEMEHL (50). Calculation of methylation frequency by SEGEMEHL is done as CpG/(CpG+TpG). Next, the data were corrected for partial deamination. Intrinsic CpT dinucleotides in the context of the motifs TGTGGGTTCTATAGATATGA (amplicon Nr−29), TATTGGGTAGCTTTTAAGTTTT (Nr−01), TTTAGAGATTCTTATTAAAGGT (Nr−00), and AATGGCTGGTAT (IH-ICR) were selected and used to search the data sample-wise. Nonconversion rate r = CpT/(CpT + TpT) was determined, then averaged for the four motifs and finally applied in the sample data to correct methylation frequency for incomplete deamination: $MF_{corr} = (MF - r)/(1 - r)$ (67).

Statistical Analysis

Principal component analyses were performed on the combined methylation data for all analyzed *Nr3c1* CpGs together and for each of the six amplicons separately. These were performed on CpG-wise

Table 3. *Nr3c1 and Igf2/H19 ICR amplicons*

Amplicon	Target	Amplicon Size, bp	Genomic Positions	CpGs, *n*
Nr−29	Exon 1_1	223	Chr18: 32,703,429–32,703,207	4
Nr−01	5′-end of CGI	176	Chr18: 32,675,231–32,675,056	11
Nr−00	Center of CGI	199	Chr18: 32,673,819–32,673,621	17
Nr+01	3′-CGI Shore	251	Chr18: 32,672,137–32,671,887	6
Nr+02	3′-CGI Shore	290	Chr18: 32,671,188–32,670,899	5
IH-ICR	*Igf2/H19* ICR	148	Chr1: 215,749,356–215,749,209	6

Genomic positions taken from Rat Genome version: July 2014 (RGSC 6.0/rn6). Amplicon size: for information on primer sequences see supplementary material. Note that *Nr3c1* is located on the opposite strand of the reference genome sequence. ICR, imprinting control region.

Table 4. *Primer sequences (first and second PCR) of the analyzed Nr3c1 and Igf2/H19 ICR amplicons*

Amplicon	Forward Primer (First PCR)*	Reverse Primer (First PCR)*	Product Size (First PCR)	Forward Primer (Second PCR)†	Reverse Primer (Second PCR)†
Nr−29	ATAATTGGTGTAGGGATAGGTG	TAAAACTCAAAATTCTACTTACCTTC	227	ATTGGTGTAGGGATAGGTGTAG	AACTCAAAATTCTACTTACCTTCATC
Nr−01	TAAGATGGTTGTTTGGATTTTATG	ATAACTTTTACTCCCCACAAATAC	411	GTTGTTTTGGATTTTATGGAGGTAG	ATCACCATCTTAACAAAAATACTCTT
Nr−00	GTTTTTTTTTTTAGGTTTTTTTTAGAGGG	TCTTTAATTTCTCTTCTCCCAAACT	288	ATTTTGTAGTTTTTTTGTTAGTGTGATA	TCTTTAATTTCTCTTCTCCCAAACT
Nr+01	TAGTTTTATATTTTAAGATTTTGGGTAAG	CCTATAAAAAACTTCTCTCTCAAAAC	256	TTTTATTATTTTAAGATTTTGGGTAAGGTT	TATAAAAAACTTCTCTCTCAAAACCC
Nr+02	GGAGGAATTTTGAAAGGTTTAGAA	CACAAAAACAACAAAATTACATTAAAC	326	TGAAAGGTTTAGAAGTGTTGGGA	CAACTAAATTTAACTATTTATCCTATCAC
IH-ICR	GGTTGTATATTGAAATTAGAGAATTTG	CCATAAATAAACCCGAACTTTAATC	148	GGTTGTATATTGAAATTAGAGAATTTG	CCATAAATAAACCCCAACTTTAATC

*Primer sequence are from 5′- to 3′-direction. †Amplicon size and number of CpGs are given in Table 3.

centered methylation data. The first and the second principal component are shown.

Pairwise correlation analyses were conducted between all samples on the combined methylation data of all analyzed CpGs separately for *Nr3c1* and *Igf2/H19* ICR (Pearson correlation). The resulting correlation matrix includes the methylation data of all samples.

The amplicon-specific methylation profiles were analyzed in a comparative regression analysis (15). They were modeled in two different ways. A global regression model was fitted to all available data per amplicon. It was compared with a pair of group-wise models fitted to the data of the respective groups. The significance of a difference between the two groups was determined by a comparison of the least square errors of the global model and the pair of individual models (F-test) (37, 46). The results were corrected for multiple testing via the false discovery rate (FDR) method and the threshold for statistical significance was set at FDR <0.05.

Individual models were chosen according to the Akaike information criterion (2). They were selected from a set of 10 predefined model types. The CuCompare software is available at http://sysbio.uni-ulm.de/soft/CuCompare.

The comparative regression analysis is designed for testing two-sided hypotheses. That is, it basically indicates the significance of the difference between the group-wise regression models but not an overall tendency of the group-wise methylation rates (e.g., higher/lower methylation in *group A* than in *group B*). We extract this information from a CpG-wise comparison of the resulting regression models. It is quantified in form of a score S

$$S = (N_A - N_B)/(N_A + N_B).$$

Here N_A and N_B denote the number of CpGs for which the regression model of *group A* or *B* achieve a higher methylation rate than the other group. A value of $S = 1$ indicates that the model of *group A* predicts a higher methylation rate than the model of *group B* for each of the CpGs in the amplicon. For $S = -1$, lower methylation rates are predicted for all CpGs of *group A*.

All statistical analyses were performed in R, version 3.3.1 (54).

Transcriptome Data Mining

Liv and Ski samples were obtained from 6 ($n = 4$) and 24 ($n = 5$) mo old male rats. All animals were housed and euthanized in compliance with national and state regulations. Purification of RNA was done using Qiagen RNeasy Mini Kit. RNA-Seq was performed using Illumina HiSeq 2500 with 50 nt single read technology and a sequencing depth of at least 20 million reads/sample. Reads were aligned against the RefSeq mRNA catalog using bwa aln (-n 2 -o 0 -e 0 -O 1000 -E 1,000) (32). P values for differential expression of genes were determined with DESeq2 (39). As the expression of only three genes was considered, nominal P values were used for data interpretation. The RNA-Seq data have been deposited at the Gene Expression Omnibus (GEO) database under the SuperSeries accession number GSE103066.

RESULTS

BS Amplicon Sequencing

The rat *Nr3c1* promoter structure comprises a distal and a proximal promoter region, positioned ~30 and 5 kb upstream of the translational start site in exon 2, respectively (44, 61). At least one distal and eight proximal untranslated first exons have been annotated. The eight first exons 1_{4-11} in the proximal region lie within a CGI that spans ~3 kb. We analyzed five loci (amplicons) along the promoter (Fig. 1). They are named according to their distance from the center of the CGI: Nr−29, Nr−01, and Nr−00 (29, 1, and 0 kb upstream); Nr+01 and Nr+02 (1 and 2 kb downstream). The *Igf2/H19* ICR amplicon is named IH-ICR. Table 3 shows detailed specification of all amplicons. Altogether we determined the methylation of 49 CpGs.

BS Amplicon-seq was performed for seven tissues (Cor, Hip, Hyp, Pit, Adr, Ski, Liv) in eight males and eight females at each of three age points (3, 9, and 24 mo). On average 2,565,327 (1,121,385–4,986,664) total reads were obtained per animal. From these, 37.1% (22.3–45.8%) met the filtering criteria (see MATERIALS AND METHODS). Read numbers analyzed per amplicon and sample have a median of 21,236 (1,181–228,071; Fig. 2).

Methylation is Locus and Tissue Specific

Figure 3 provides an overview of the observed methylation patterns and indicates a complex interplay of amplicon-, tissue-, sex-, and age-specific effects. Most obviously, the amplicons showed different levels of methylation. Average methyl CpG rates were very high (0.8–0.96) for Nr−29. Nr−01 located at the 5′-end of CGI has decreasing methylation rates from CpG 1 to 11 (0.19–0.0). Nr−00 CpGs located at core of the CGI showed very low CpG methylation rates; among these, CpGs 9 and 11 showed highest methylation (0.0–0.03 and 0.02–0.05, respectively). Amplicons located at the 3′-shore of the CGI showed increasing methylation rates with increasing distance away from the CGI (Nr+01: 0.0–0.4; Nr+02: 0.07–0.93). IH-ICR a locus where both a highly methylated and an unmethylated allele can be expected has methylation rates of 0.3–0.49. The overview of the methylation patterns in these loci provides the first evidence for tissue specificity: e.g., methylation at Nr+01/+02 in Pit and Adr are higher than in the other tissues (Fig. 3).

To examine the tissue specificity of the methylation patterns of *Nr3c1* and *IH-ICR* in more detail, we performed principal component analyses. It showed that tissue-specific methylation of *Nr3c1* explains most of the methylation variation between samples (Fig. 4*A*). A "hierarchical" order can be observed for brain tissues and tissues composing the HPA axis (Cor-Hip-Hyp-Pit-Adr) along principal component 1 (abscissa). At the level of single amplicons, tissue specificity was most pronounced at Nr+01/+02 (3′-CGI shore, Fig. 5, *D* and *E*) and absent at Nr−00 (CGI core, Fig. 5*C*) and IH-ICR (Fig. 5*F*). Minor tissue specificity was found at Nr−29 (skin vs. remain-

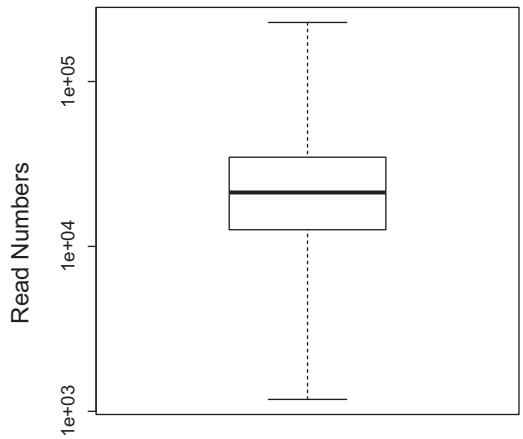

Fig. 2. Number of reads analyzed per sample. The boxplot shows the median, 2nd/3rd quartiles (box), and minimum/maximum (whiskers).

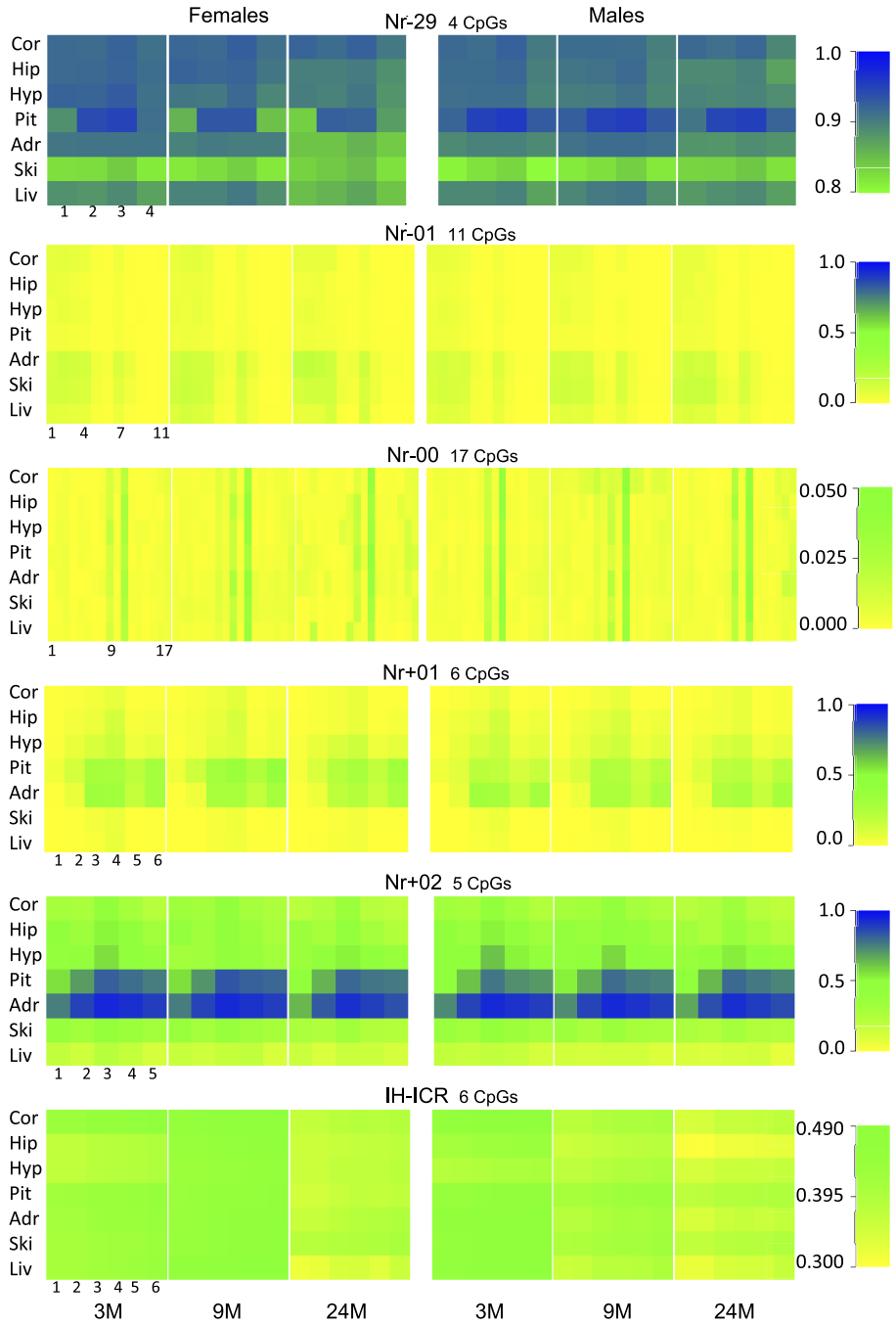

Fig. 3. Overview of the identified methylation patterns of the *Nr3c1* and *Igf2/H19* imprinting control region (ICR) amplicons with respect to tissue, sex, and age. Main columns, age [in months (M)]; subcolumns, CpGs; rows, tissues (Cor, cortex; Hip, hippocampus; Hyp, hypothalamus; Pit, pituitary; Adr, adrenal cortex; Ski, skin; Liv, liver); cell color, methylation rate of single CpG (mean of 8 rats). Note that color scales are amplicon specific. Numbering of CpGs is shown in the *left* main column.

ing tissues, Fig. 5*A*) and Nr−01 (Adr, Ski, and Liv vs. brain tissues; Figs. 3 and 5*B*).

Pairwise correlation analysis of methylation levels of the individual CpGs between all samples confirmed the tissue specificity at *Nr3c1* and its absence at IH-ICR (Fig. 4*B*). The correlation of methylation levels within and between tissues was in general considerably higher for *Nr3c1* than IH-ICR (median: 0.96 vs. 0.87; $P < 0.001$, Wilcoxon rank test), indicating higher plasticity and stochastic fluctuations of methylation at this ICR. Moreover, correlation significantly decreased with age at both loci (Fig. 4, *C* and *D*), consistent with an accumulation of noise over time. Pairwise correlations between tissues at *Nr3c1* (Fig. 4*B*) were highest among Pit and Adr (median: 0.99) as well as among Cor, Hip, Hyp, and Ski (median: 0.98). The latter indicates that Ski methylation, as a readily accessible tissue, may serve as proxy for *Nr3c1* methylation in brain tissues. Within the same animal the correlation between Cor, Hip, Hyp, and Ski was even higher (median: 0.99, Fig. 4*E*). Among the individual *Nr3c1* amplicons Nr+01 showed the highest correlation (Figs. 4*F* and 6).

Sex-specific Methylation Changes during Aging

The principal component analyses also provided the first evidence for a sex-specific methylation as Pit and Adr show a

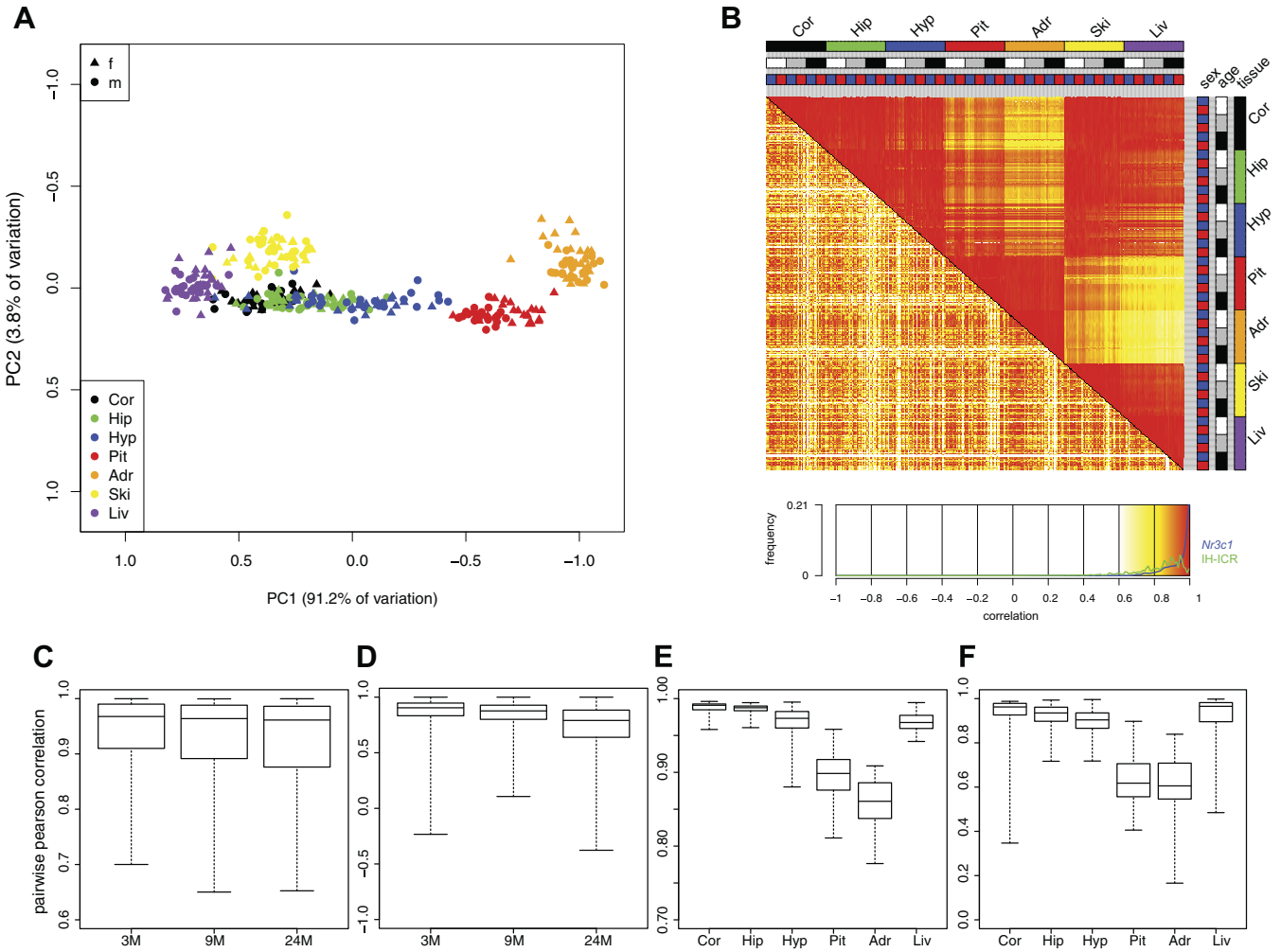

Fig. 4. Tissue-specific methylation. *A*: principal component analyses of *Nr3c1* data stratified by tissue (color) and sex (shape). Each data point represents the methylation data of 1 tissue of 1 animal. *B*: pairwise Pearson correlation between all samples on the combined methylation data of all analyzed CpGs for *Nr3c1* (upper right triangle) and IH-ICR (lower left triangle). Samples are presorted by tissue (1st level: colors top/right), age (2nd level: white, 3 mo; gray, 9 mo; black, 24 mo) and sex (3rd level: blue, females; black, males). Boxplots of all correlation coefficients per age groups for *Nr3c1* (*C*) and IH-ICR (*D*). All pairwise comparisons are significantly different ($P < 0.001$, Wilcoxon rank test). Boxplots of *Nr3c1* correlation coefficients between Ski and the other tissues of the same animal based on all analyzed CpGs (*E*) and on Nr+01 CpGs (*F*). Tissues: Cor, cortex; Hip, hippocampus; Hyp, hypothalamus; Pit, pituitary; Adr, adrenal cortex; Ski, skin; Liv, liver. M, months.

tendency for separation of male and female samples (Figs. 4*A* and 5*D*). To further assess sex-specific differences in methylation patterns, we performed CuCompare analyses (males vs. females) for each amplicon per tissue and age group (126 comparisons) (Fig. 7). Over all tissues and amplicons, 12, 21, and 10 significant differences (FDR <0.05) were observed at 3, 9, and 24 mo, respectively (Fig. 7, *A* and *B*). In both *Nr3c1* and IH-ICR loci, sex specificity appears at all ages but peaks at 9 mo (Fig. 7*C*, Table 5). The fewest sex differences were observed at 24 mo for IH-ICR.

In *Nr3c1*, sex-specific methylation occurred in all tissue in at least two amplicons and one time point (Fig. 7*A*). Most sex differences were observed in Pit, where, except for Nr−00, all loci showed sex specificity in 10 out of 12 comparisons. Remarkably, Nr−29 methylation levels were consistently greater in males than in females over the entire lifespan, while Nr+01 showed the opposite relation between sexes. A direction change of the methylation difference was observed at Nr−29 in Adr: at 3 mo, methylation levels in females were greater than in males, while at 9 and 24 mo, levels in females were less than in males (Fig. 7*A* and Supplemental Fig. S1A) due to hypomethylation in females at 24 mo (Supplemental Fig. S2A) and hypermethylation in males at 9 mo (Supplemental Fig. S3A). (The online version of this article contains supplemental material.)

For the IH-ICR, methylation of Hip, Adr, and Ski was higher in males than in females at 3 mo (Fig. 7*A*). This direction of the sex-specific difference changed with age. At 9 mo, the methylation level of all tissues was higher in females than in males. At 24 mo, only Hip maintained the 9 mo sex specificity, while all other tissues showed no significant sex-specific methylation differences.

As we observed age-dependent sex-specific methylation, we analyzed methylation changes with age separately by sex (Fig. 8). Pairwise CuCompare tests between time points for each tissue/amplicon showed sex-specific methylation changes during aging in most gene loci and tissues. The *Nr3c1* mostly showed hypermethylation of Nr−01 and Nr−00, located in the CGI, while amplicons located outside of the CGI became largely hypomethylated with age (Fig. 8, *A* and *B*). The latter

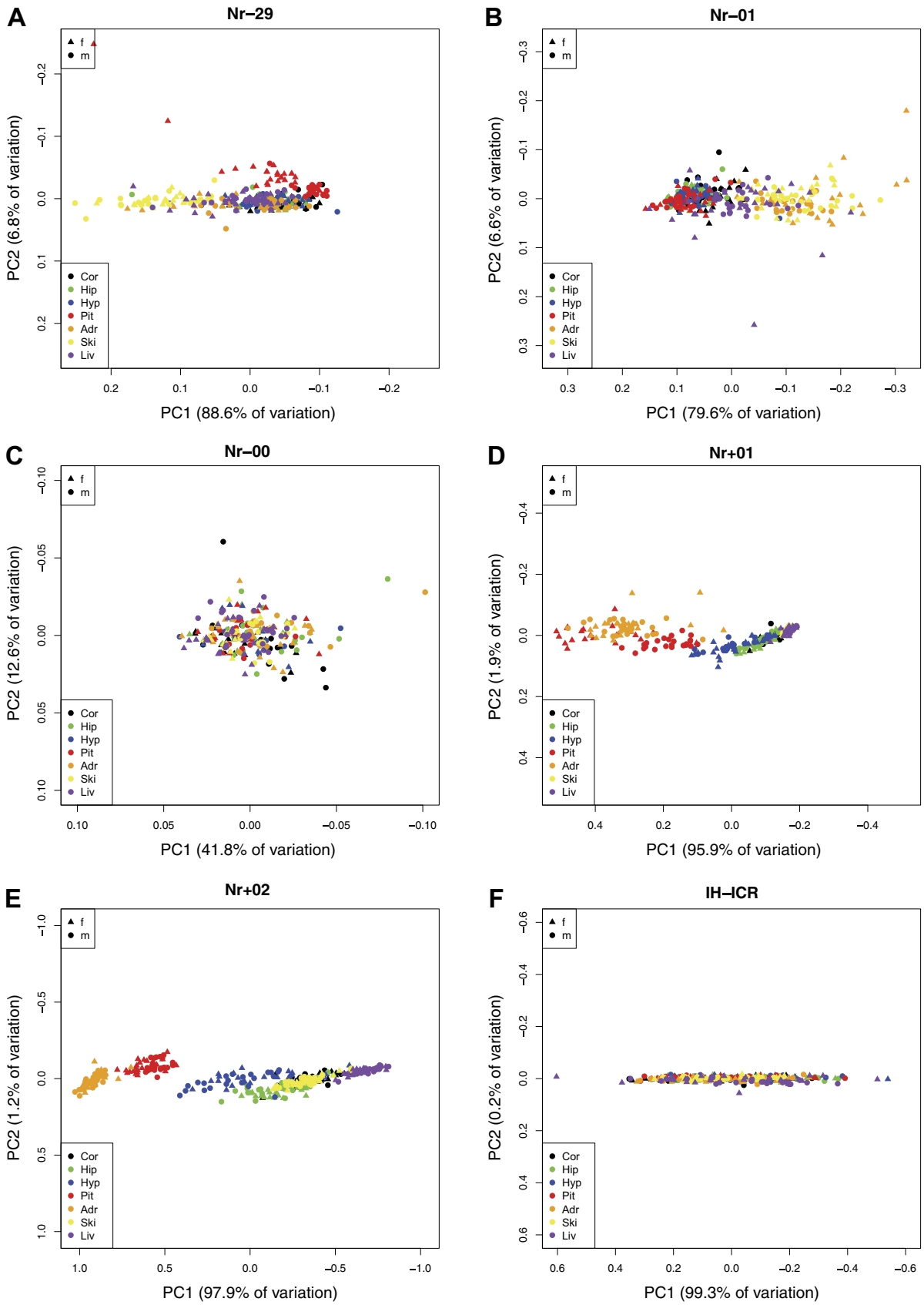

Fig. 5. Principal component analyses of individual amplicons stratified by tissue (color) and sex (shape). *A*: Nr−29, *B*: Nr−01, *C*: Nr−00, *D*: Nr+01, *E*: Nr+02, *F*: IH-ICR. Each data point represents methylation data of the respective amplicon per tissue and animal.

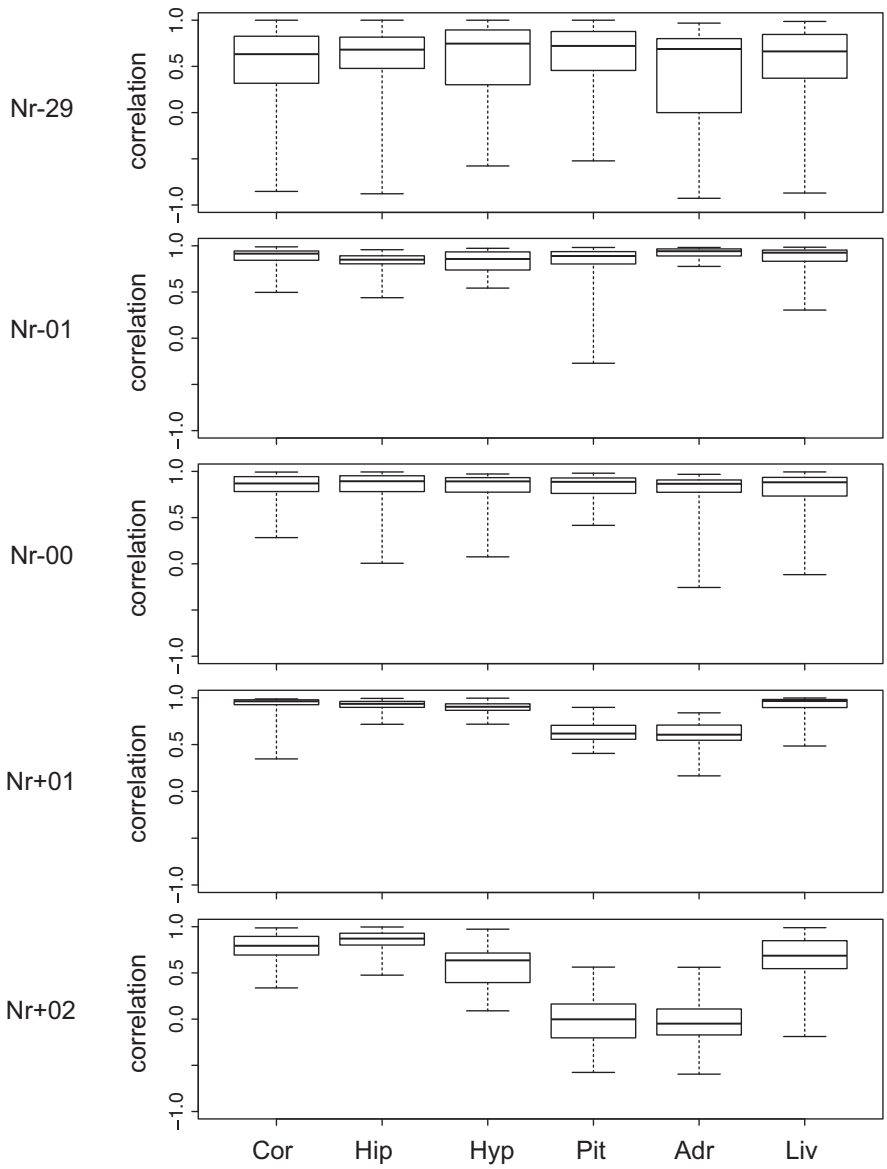

Fig. 6. Boxplots of *Nr3c1* correlation coefficients between Ski and the other tissues of the same animal based on all analyzed CpGs per respective amplicon Nr−29, Nr−01, Nr−00, Nr+01, and Nr+02. Tissues: Cor, cortex; Hip, hippocampus; Hyp, hypothalamus; Pit, pituitary; Adr, adrenal cortex; Ski, skin; Liv, liver.

was more prominent in females. Only in eight out of 35 comparisons between time points similar methylation changes occurred in both sexes: Nr+02 (Liv) showed continuous hypomethylation over the lifespan; Nr+01 (Hip) and Nr+02 (Cor and Adr) hypomethylation after 9 mo; Nr−29 (Cor and Ski), Nr−01 (Hyp), and Nr+01 (Cor) showed no age-related methylation changes.

The *Igf2/H19* ICR became predominantly hypomethylated during aging. This was more pronounced in males than in females (Fig. 8, Table 6). Males showed a continuous decrease in methylation with age in all tissues after 3 mo except in Hyp and Pit, which showed a decrease only after 9 mo. Methylation in females decreased in Cor, Pit, and Adr after 9 mo. In Hip, Hyp, Ski, and Liv it followed a peak-shaped curve during aging as methylation levels were highest at 9 mo.

Methylation and Transcript Level Changes during Aging are Associated

To get an initial idea whether the observed significant changes of methylation levels during aging can be mechanistically linked to respective changes at the transcript level, we mined transcriptome data of Liv and Ski of 6 and 24 mo old male rats for *Nr3c1*, *Igf2,* and *H19* expression. These data indicate that the expression levels as well as their changes during aging are highly gene and tissue specific (Table 7).

Remarkably, *Nr3c1* transcript levels in Ski increase significantly with age ($P = 0.03$, DESeq2), in line with a highly significant hypomethylation of Nr+02 over the lifespan (Fig. 8). On the other hand, in liver, the *H19* vs. *Igf2* expression ratio significantly increases ($P < 0.02$, Wilcoxon rank sum test), in parallel to the highly significant hypomethylation of IH-ICR during aging (Fig. 8).

DISCUSSION

The specific methylation patterns of *NR3C1* and *IGF2/H19* ICR and their changes over the lifespan are of particular interest since these genes are prone to epigenetic modifications and they are important in the control of development, aging and disease processes. As DNA methylation is variable and

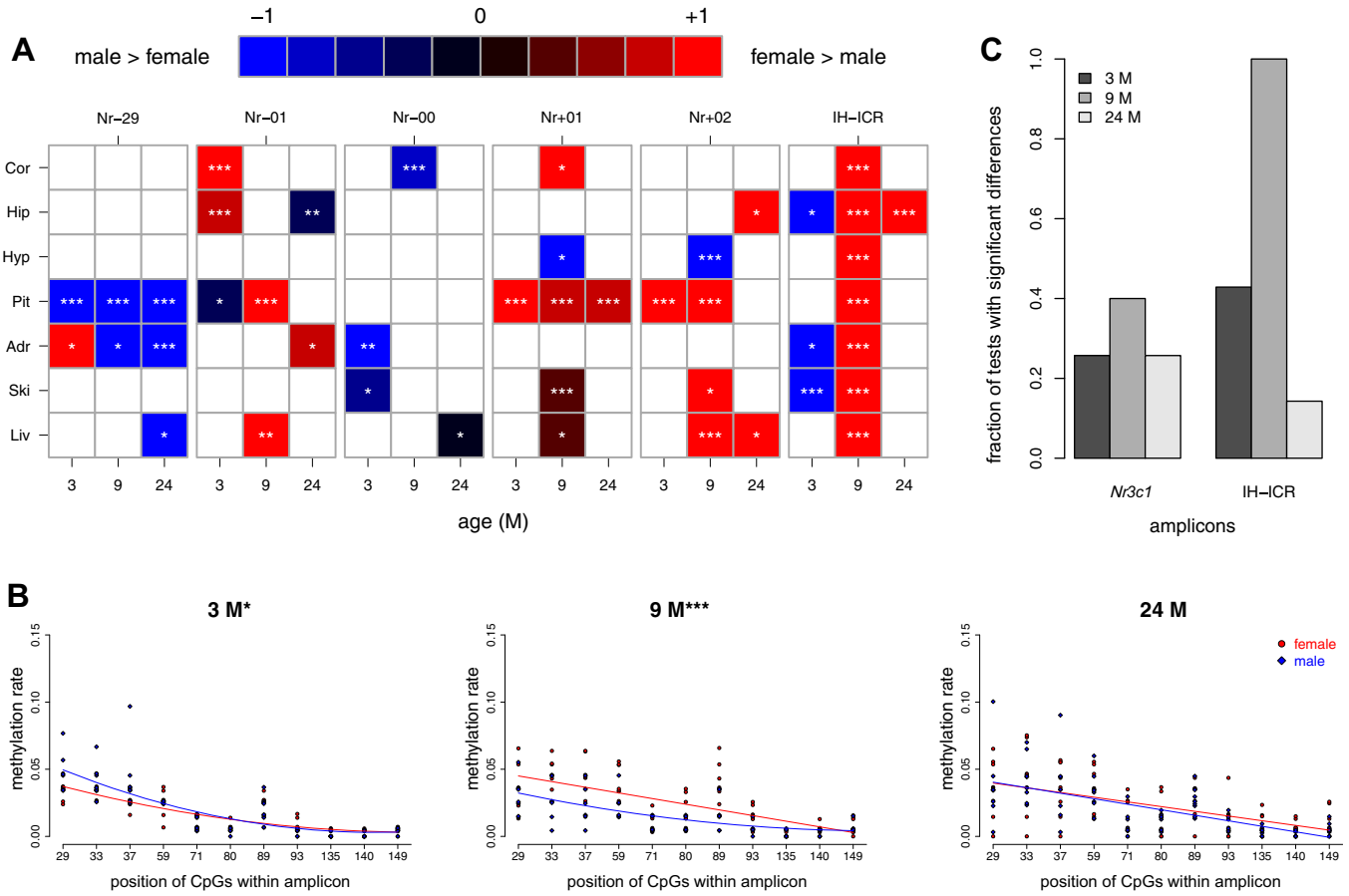

Fig. 7. Sex-specific methylation of *Nr3c1* and IH-ICR amplicons. *A*: heat map of sex differences. Columns, amplicons age-wise; rows, tissues (Cor, cortex; Hip, hippocampus; Hyp, hypothalamus; Pit, pituitary; Adr, adrenal cortex; Ski, skin; Liv, liver). Color scale: quantification of the directionality of sex difference (see MATERIALS AND METHODS). All CuCompare plots used for heat map generation are provided as supplementary figures (Supplemental Fig. S1). *B*: example of CuCompare plots for the methylation rate of the Nr−01 amplicon obtained from the pituitary at all 3 ages. *C*: fractions of tests exhibiting significant methylation differences for the 3 ages (Table 5). $*P < 0.05$, $**P < 0.01$, $***P < 0.001$; false discovery rate (FDR) by CuCompare analysis. M, months.

dependent on a variety of factors, many human and animal studies focusing on these loci in different tissues, sexes, and ages may not be comparable.

To provide a comprehensive base for future experimental studies in rats as an established model organism, we characterized DNA methylation patterns of different *Nr3c1* promoters and *Igf2/H19* ICR in seven tissues and at three age points. Since in humans most tissues such as brain are not readily accessible and proxy materials have to be analyzed instead, we investigated in particular whether there is correlation of methylation between tissues in the rat.

Table 5. *Methylation differences between sexes*

	Amplicons						
	Nr3c1						*Igf2/H19* ICR
Age, mo	Nr−29	Nr−01	Nr−00	Nr+01	Nr+02	Total*	IH-ICR*
3	2	3	2	1	1	9	3
9	2	2	1	5	4	14	7
24	3	2	1	1	2	9	1

Numbers of significant CuCompare tests (FDR <0.05) between sexes were summarized over all tissues per amplicon and age (Fig. 7*A*, Supplemental Fig. S1). *Numeric basis for histogram Fig. 7*C*.

Methylation of Nr3c1

In agreement with general methylation patterns in humans (16), we found that rat *Nr3c1* shows high methylation levels at shores of the CGI and the distal promoter, while low levels occur within the island. The methylation analysis of this gene is particular demanding, as its promoter structure in mammals is highly complex, although conserved between humans and rats (62). Most DNA methylation studies of rat *Nr3c1* have focused on the exon 1_7 promoter homologous to 1F in human. Only a few studies have looked at other human promoters in the CGI such as 1B, IC, 1D, IE, and IH (11, 51, 63). Our study is the first analysis of DNA methylation in the *Nr3c1* exon 1_1, exon 1_4 promoter at the 5′-end of the CGI and at the 3′-CGI shore of the rat.

Tissue specificity. DNA methylation levels vary among tissues especially at non-CGI regions of the genome (36). We observed that tissue-specific methylation in *Nr3c1* is most pronounced at the 3′-CGI shore where methylation levels were high (Figs. 4*A* and 5). The importance of CGI shores for health and disease is recently becoming clearer; Irizarry et al. (24) showed that tissue-specific methylation mostly occurs there and not within CGIs, and methylation changes in colon cancer accumulate commonly there. In agreement with this study,

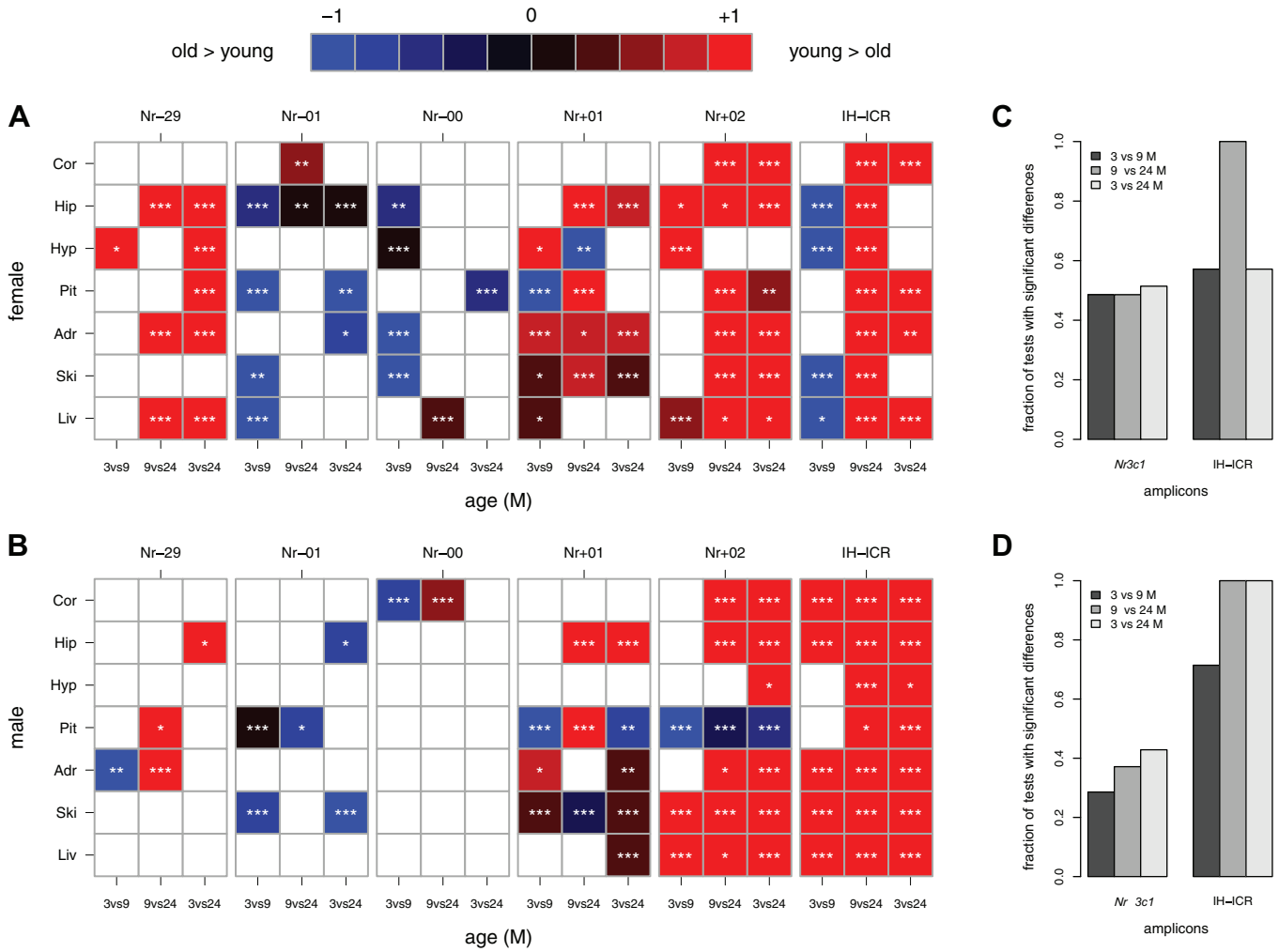

Fig. 8. Age-specific methylation of *Nr3c1* and IH-ICR amplicons. Heat maps of age differences in females (*A*) and males (*B*). Columns, pairwise comparisons of ages per amplicon; rows, tissues (Cor, cortex; Hip, hippocampus; Hyp, hypothalamus; Pit, pituitary; Adr, adrenal cortex; Ski, skin; Liv, liver). Color scale: quantification of the directionality of age difference (see MATERIALS AND METHODS). All CuCompare plots used for heat map generation are provided as supplementary figures (Supplemental Fig. S2, female data; Supplemental Fig. S3, male data). Fractions of age pairs exhibiting significant methylation differences in all *Nr3c1* (*C*) and IH-ICR (*D*) amplicon (Table 6). Significance levels: *<0.05, **<0.01, ***<0.001; FDR by CuCompare analysis. M, months.

Nr−00 located at the core of the CGI lacks tissue-specific methylation (Fig. 5*C*). It also showed lowest methylation levels among all amplicons in all tissues in accordance with previous knowledge that CGIs are usually hypomethylated (16). Methylation of Nr−01 at the 5′-end of the CGI and Nr−29 at the distal promoter showed minor tissue specificity (Figs. 3 and 5, *A* and *B*). Strikingly, CpGs 1–4 and 7 in NR−01 are more highly methylated in nonbrain tissues (Adr, Ski, and Liv) than in brain tissues (Fig. 3). CpGs 1–4 are closest to the 5′-end of the CGI; the 1st CpG of Nr−01 marks the 5′-end of the CGI. At the distal promoter (Nr−29) Ski showed lowest methylation levels compared with other tissues (Fig. 3).

Our finding that methylation of *Nr3c1* correlated highly in skin and brain tissues including Hip and Hyp, which are the central parts of the HPA axis, is of particular interest. Skin biopsies are easily accessible in humans. Further studies are required to show whether epigenetic modifications in the skin may serve as proxy for assessment of vulnerability to stress- and aging-associated diseases. In this context it seems worthwhile to refer to a number of studies correlating in humans *NR3C1* methylation changes in blood mononuclear cells with depression (8).

Sex specificity. Various studies have shown genome-wide DNA methylation differences between sexes (34, 43). With respect to the *NR3C1* promoter and *IGF2/H19* ICR, sex-specific methylation changes were reported for infants in response to prenatal stress exposure (42, 49). Moreover, in 4 mo old offspring from mice exposed to several prenatal stressors, a correlation of sex-specific *Nr3c1* methylation and expression was shown (47). However, no study has investigated sex-specific methylation changes of the *NR3C1* promoter and *IGF2/H19* ICR during aging. We found, at both loci, sex specificity of methylation in all investigated rat tissues for at least one time point, which peaked at 9 mo. This correlates with the differential expression pattern of sex hormones during the lifetime: rising from puberty, being most pronounced at adolescence, and declining with aging (3, 10, 20). Depending on the locus and tissue, we observed losses, gains, and the inversion of sex-specific methylation during aging. These complex sex-specific trajectories of methylation during develop-

Table 6. *Methylation differences between ages*

Age Comparison, pairwise	Amplicons						
	Nr3c1						*Igf2/H19* ICR
	Nr−29	Nr−01	Nr−00	Nr+01	Nr+02	Total*	IH-ICR*
				Female			
3 vs. 9 mo	1	4	4	5	3	17	4
9 vs. 24 mo	3	2	1	5	6	17	7
3 vs. 24 mo	5	3	1	3	6	18	4
				Male			
3 vs. 9 mo	1	2	1	3	3	10	5
9 vs. 24 mo	2	1	1	3	6	13	7
3 vs. 24 mo	1	2	0	5	7	15	7

Numbers of significant pairwise CuCompare tests (FDR <0.05) between ages were summarized over all tissues per amplicon and sex (Fig. 8, *A* and *B*; Supplemental Figs. S2 and S3). *Numeric basis for histogram Fig. 8, *C* and *D*.

ment and aging need to be considered for the design, interpretation, and comparison of experimental and clinical studies.

Among all amplicons and tissues only Nr−29 (exon 1_1) and Nr+01 (3′-CGI shore) in Pit showed a continuous sex-specific methylation difference at the 3–24 mo time period. The methylation was higher at Nr−29 in males and at Nr+01 in females (Fig. 7*A* and Supplemental Fig. S1, A and D). This may indicate that in Pit a subset of neuroendocrine cells related to HPA axis function stably utilizes the complex *Nr3c1* promoter in a sex-specific manner.

Age specificity. In all tissues regardless of sex, we observed a general tendency of decreasing methylation levels at *Nr3c1* with age. This observation is consistent with studies showing that DNA methylation decreases in aging (1, 65). Genome-wide studies confirming the general hypomethylation during aging have shown, however, that hypermethylation occurs at CpGs located within CGIs (22, 25, 26). We also observed that hypermethylation during aging occurred more often in Nr−01 and Nr−00 located within CGI, while a high incidence of hypomethylation was observed mostly at the 3′-CGI shore amplicons (Nr+01 and Nr+02) and the Nr−29 amplicon. In agreement with previous studies (12, 40), age-related methylation changes were not only tissue specific but also locus specific. By analyzing six amplicons along the promoter of *Nr3c1* in seven tissues, we observed that both sexes only have few similar age-specific methylation changes: continuous hypomethylation in Nr+02 (Liv) and hypomethylation after 9 mo in Nr+01 (Hip), Nr+02 (Cor and Adr), and IH-ICR (Pit). Moreover in both sexes methylation remained unchanged over the lifespan at Nr−29 (Cor and Ski), Nr−01 (Hyp), and Nr+01 (Cor). In contrast, the remaining loci/tissues showed methylation changes during aging that were sex specific.

With respect to *Nr3c1* expression, a global study showed that high methylation of CGI shores is associated with high gene expression (16). Whether the aging-related hypomethylation observed at the *Nr3c1* shore affects expression is a question for future studies. It will also be interesting to see whether the expression of the alternative first exons of *Nr3c1* is differently or concordantly affected by methylation changes at the CGI shores. In relation to glucocorticoid receptor expression in tissues during aging, studies from the literature are contradictory. Earlier studies showed that glucocorticoid receptor expression declines with aging in different tissues of rat and human (7). Similarly, another study found that *Nr3c1* mRNA was decreased in the Hip of aged rats (21). In contrast, *NR3C1* mRNA was increased in human prefrontal cortex but not in Hip during adolescence and adulthood compared with infancy and older age (52). The complexity of the *NR3C1* expression is most likely related to the fact that it has multiple first exons that can be utilized differentially among tissues and over time (53, 62). Further studies of the *NR3C1* expression are needed to better understand the role of the glucocorticoid receptor in aging.

As a step in this direction, we observed in male rat Ski an association of Nr+02 hypomethylation and increased *Nr3c1* transcript levels during aging. Mechanistically, this would fit the scientific consensus of an anticorrelation between promoter methylation and expression (27). The fact that in Liv a similar Nr+02 hypomethylation was not accompanied by *Nr3c1* transcript levels remained constant again emphasizes the complexity of the *Nr3c1* expression mentioned above and the need for further investigations.

Methylation of Igf2/H19 ICR

The *Igf2/H19* ICR did not show tissue-specific DNA methylation, but similar to *Nr3c1*, we found sex- and age-specific patterns. Opposite to *Nr3c1*, hypomethylation with age was more prominent in males than in females. The latter displayed a peak-shaped methylation curve during aging in Hip, Hyp, Ski, and Liv. Males showed a continuous decrease in methylation levels in Cor, Hip, Adr, Ski, and Liv. Altogether, *Igf2/H19* ICR methylation levels declined from 9 to 24 mo in all tissues of both sexes. There is evidence indicating that hypomethylation of the *Igf2/H19* locus, which leads to downregulation of *Igf2* and upregulation of *H19* expression, plays an important role in regulating quiescence of pluripotent stem cells in adult organisms and may be involved in

Table 7. *Transcript level changes of Nr3c1, Igf2, and H19 during aging in male rat liver and skin*

	Liver							Skin						
	RPKM				HIER			RPKM				HIER		
	6 mo	24 mo	TLC	*P*	6 mo	24 mo	*P*	6 mo	24 mo	TLC	*P*	6 mo	24 mo	*P*
Nr3c1	23.17	18.02	−0.36	0.27				23.32	36.54	0.65	0.03			
Igf2	0.34	0.33	−0.06	0.96	2.16	5.95	0.02	4.02	7.21	0.85	0.04	126.45	116.47	1
H19	0.74	1.96	1.40	2×10^{-9}				499.84	958.21	0.94	0.13			

Reads per transcript kb and million reads (RPKM) are means across replicates. Transcript level changes (TLC) are $\log_2$(24 mo/6 mo). TLC nominal *P* value were obtained by DESeq2. *H19* vs. *Igf2* expression ratio (HIER) is the mean of the ratios calculated for each animal separately. *P* values for HIER differences between 6 and 24 mo were obtained by Wilcoxon rank sum test.

the regulation of lifespan. In contrast, hypermethylation of this locus results in Igf2 overexpression and is observed in several malignancies (55).

Mechanistically, the observed association of IH-ICR hypomethylation and increased *H19/Igf2* expression ratio during aging in male rat Liv fits the scientific consensus of the role of this element as a DNA methylation-dependent enhancer-blocking insulator (5). The fact that a similar shift of the expression ratio was not seen in Ski despite hypomethylation of IH-ICR indicates tissue-dependent differences in the regulation of the two genes, consistent with the high tissue specificity of their expression observed by us and others (https://www.ebi.ac.uk/gxa).

In conclusion, our study characterizes the DNA methylation changes that take place during aging in rats by using a locus-specific BS Amplicon-seq approach in multiple tissues for *Nr3c1* promoter and *Igf2/H19* ICR. Our results provide a reference for further studies on the role of DNA methylation of the two loci in aging and disease.

ACKNOWLEDGMENTS

We thank Institute of Laboratory Animal Science and Welfare at the Jena University Hospital for animal upkeep, Cornelia Luge and Beate Szafranski for laboratory assistance, Andrew Heidel for providing the primer tags, Philipp Koch for technical support, and Debra Weih for critical reading of the manuscript.

GRANTS

The research was financially supported by the European Community's Seventh Framework Programme (FP7-HEALTH-2012-279281).

DISCLOSURES

No conflicts of interest, financial or otherwise, are declared by the authors.

AUTHOR CONTRIBUTIONS

M.S., O.W.W., and M.P. designed the experiments. O.B.A., K.H., C.B., M. Groth, and M. Gall performed experiments; O.B.A., L.L., K.H., N.J., M.B., A.S., H.A.K., and M.P. analyzed data; O.B.A., L.L., K.H., M.S., and M.P. interpreted results of experiments; O.B.A., L.L., and H.A.K. prepared figures; O.B.A., L.L., H.A.K., M.S., and M.P. drafted manuscript; O.B.A., L.L., K.H., C.B., N.J., M. Groth, M.B., A.S., M. Gall, O.W.W., H.A.K., M.S., and M.P. approved final version of manuscript.

The manuscript was prepared and written with contributions from all authors. All authors have approved the final version of the manuscript and agree to be accountable for all aspects of the work. All persons designated as authors qualify for authorship, and all those who qualify for authorship are listed.

REFERENCES

1. **Aguilera O, Fernández AF, Muñoz A, Fraga MF.** Epigenetics and environment: a complex relationship. *J Appl Physiol (1985)* 109: 243–251, 2010. doi:10.1152/japplphysiol.00068.2010.
2. **Akaike H.** A new look at the statistical model identification. *IEEE Trans Automat Contr* 19: 716–723, 1974. doi:10.1109/TAC.1974.1100705.
3. **Apter D.** Serum steroids and pituitary hormones in female puberty: a partly longitudinal study. *Clin Endocrinol (Oxf)* 12: 107–120, 1980. doi:10.1111/j.1365-2265.1980.tb02125.x.
4. **Bartolomei MS, Zemel S, Tilghman SM.** Parental imprinting of the mouse H19 gene. *Nature* 351: 153–155, 1991. doi:10.1038/351153a0.
5. **Bell AC, Felsenfeld G.** Methylation of a CTCF-dependent boundary controls imprinted expression of the Igf2 gene. *Nature* 405: 482–485, 2000. doi:10.1038/35013100.
6. **Cao-Lei L, de Rooij SR, King S, Matthews SG, Metz GAS, Roseboom TJ, Szyf M.** Prenatal stress and epigenetics. *Neurosci Biobehav Rev* 2017, Epub ahead of print. doi:10.1016/j.neubiorev.2017.05.016.
7. **Chang WC, Roth GS.** Changes in the mechanisms of steroid action during aging. *J Steroid Biochem* 11, *1C*: 889–892, 1979. doi:10.1016/0022-4731(79)90025-6.
8. **Chen D, Meng L, Pei F, Zheng Y, Leng J.** A review of DNA methylation in depression. *J Clin Neurosci* 43: 39–46, 2017. doi:10.1016/j.jocn.2017.05.022.
9. **Cottrell EC, Seckl JR.** Prenatal stress, glucocorticoids and the programming of adult disease. *Front Behav Neurosci* 3: 19, 2009. doi:10.3389/neuro.08.019.2009.
10. **Cutler WB, Genovese-Stone E.** Wellness in women after 40 years of age: the role of sex hormones and pheromones. *Dis Mon* 44: 421–546, 1998. doi:10.1016/S0011-5029(98)90016-5.
11. **Daskalakis NP, Yehuda R.** Site-specific methylation changes in the glucocorticoid receptor exon 1F promoter in relation to life adversity: systematic review of contributing factors. *Front Neurosci* 8: 369, 2014. doi:10.3389/fnins.2014.00369.
12. **Day K, Waite LL, Thalacker-Mercer A, West A, Bamman MM, Brooks JD, Myers RM, Absher D.** Differential DNA methylation with age displays both common and dynamic features across human tissues that are influenced by CpG landscape. *Genome Biol* 14: R102, 2013. doi:10.1186/gb-2013-14-9-r102.
13. **de Kloet ER.** Corticosteroids, stress, and aging. *Ann N Y Acad Sci* 663: 357–371, 1992. doi:10.1111/j.1749-6632.1992.tb38679.x.
14. **DeChiara TM, Robertson EJ, Efstratiadis A.** Parental imprinting of the mouse insulin-like growth factor II gene. *Cell* 64: 849–859, 1991. doi:10.1016/0092-8674(91)90513-X.
15. **Dünkler A, Rösler R, Kestler HA, Moreno-Andrés D, Johnsson N.** SPLIFF: a single-cell method to map protein-protein interactions in time and space. *Methods Mol Biol* 1346: 151–168, 2015. doi:10.1007/978-1-4939-2987-0_11.
16. **Edgar R, Tan PP, Portales-Casamar E, Pavlidis P.** Meta-analysis of human methylomes reveals stably methylated sequences surrounding CpG islands associated with high gene expression. *Epigenetics Chromatin* 7: 28, 2014. doi:10.1186/1756-8935-7-28.
17. **Fu VX, Dobosy JR, Desotelle JA, Almassi N, Ewald JA, Srinivasan R, Berres M, Svaren J, Weindruch R, Jarrard DF.** Aging and cancer-related loss of insulin-like growth factor 2 imprinting in the mouse and human prostate. *Cancer Res* 68: 6797–6802, 2008. doi:10.1158/0008-5472.CAN-08-1714.
18. **Garrido P.** Aging and stress: past hypotheses, present approaches and perspectives. *Aging Dis* 2: 80–99, 2011.
19. **Haberman RP, Quigley CK, Gallagher M.** Characterization of CpG island DNA methylation of impairment-related genes in a rat model of cognitive aging. *Epigenetics* 7: 1008–1019, 2012. doi:10.4161/epi.21291.
20. **Harman SM, Metter EJ, Tobin JD, Pearson J, Blackman MR; Baltimore Longitudinal Study of Aging.** Longitudinal effects of aging on serum total and free testosterone levels in healthy men. *J Clin Endocrinol Metab* 86: 724–731, 2001. doi:10.1210/jcem.86.2.7219.
21. **Hassan AH, Patchev VK, von Rosenstiel P, Holsboer F, Almeida OF.** Plasticity of hippocampal corticosteroid receptors during aging in the rat. *FASEB J* 13: 115–122, 1999.
22. **Heyn H, Li N, Ferreira HJ, Moran S, Pisano DG, Gomez A, Diez J, Sanchez-Mut JV, Setien F, Carmona FJ, Puca AA, Sayols S, Pujana MA, Serra-Musach J, Iglesias-Platas I, Formiga F, Fernandez AF, Fraga MF, Heath SC, Valencia A, Gut IG, Wang J, Esteller M.** Distinct DNA methylomes of newborns and centenarians. *Proc Natl Acad Sci USA* 109: 10522–10527, 2012. doi:10.1073/pnas.1120658109.
23. **Hoal-van Helden EG, van Helden PD.** Age-related methylation changes in DNA may reflect the proliferative potential of organs. *Mutat Res* 219: 263–266, 1989. doi:10.1016/0921-8734(89)90027-1.
24. **Irizarry RA, Ladd-Acosta C, Wen B, Wu Z, Montano C, Onyango P, Cui H, Gabo K, Rongione M, Webster M, Ji H, Potash J, Sabunciyan S, Feinberg AP.** The human colon cancer methylome shows similar hypo- and hypermethylation at conserved tissue-specific CpG island shores. *Nat Genet* 41: 178–186, 2009. doi:10.1038/ng.298.
25. **Issa JP.** Age-related epigenetic changes and the immune system. *Clin Immunol* 109: 103–108, 2003. doi:10.1016/S1521-6616(03)00203-1.
26. **Johansson A, Enroth S, Gyllensten U.** Continuous aging of the human DNA methylome throughout the human lifespan. *PLoS One* 8: e67378, 2013. doi:10.1371/journal.pone.0067378.
27. **Jones PA, Takai D.** The role of DNA methylation in mammalian epigenetics. *Science* 293: 1068–1070, 2001. doi:10.1126/science.1063852.

28. **Kalimi M.** Glucocorticoid receptors: from development to aging. A review. *Mech Ageing Dev* 24: 129–138, 1984. doi:10.1016/0047-6374(84)90065-4.
29. **Kapoor A, Dunn E, Kostaki A, Andrews MH, Matthews SG.** Fetal programming of hypothalamo-pituitary-adrenal function: prenatal stress and glucocorticoids. *J Physiol* 572: 31–44, 2006. doi:10.1113/jphysiol.2006.105254.
30. **Kitraki E, Bozas E, Philippidis H, Stylianopoulou F.** Aging-related changes in IGF-II and c-fos gene expression in the rat brain. *Int J Dev Neurosci* 11: 1–9, 1993. doi:10.1016/0736-5748(93)90029-D.
31. **Koukoura O, Sifakis S, Zaravinos A, Apostolidou S, Jones A, Hajiioannou J, Widschwendter M, Spandidos DA.** Hypomethylation along with increased H19 expression in placentas from pregnancies complicated with fetal growth restriction. *Placenta* 32: 51–57, 2011. doi:10.1016/j.placenta.2010.10.017.
32. **Li H, Durbin R.** Fast and accurate short read alignment with Burrows-Wheeler transform. *Bioinformatics* 25: 1754–1760, 2009. doi:10.1093/bioinformatics/btp324.
33. **Li LC, Dahiya R.** MethPrimer: designing primers for methylation PCRs. *Bioinformatics* 18: 1427–1431, 2002. doi:10.1093/bioinformatics/18.11.1427.
34. **Liu J, Morgan M, Hutchison K, Calhoun VD.** A study of the influence of sex on genome wide methylation. *PLoS One* 5: e10028, 2010. doi:10.1371/journal.pone.0010028.
35. **Liu Y, Murphy SK, Murtha AP, Fuemmeler BF, Schildkraut J, Huang Z, Overcash F, Kurtzberg J, Jirtle R, Iversen ES, Forman MR, Hoyo C.** Depression in pregnancy, infant birth weight and DNA methylation of imprint regulatory elements. *Epigenetics* 7: 735–746, 2012. doi:10.4161/epi.20734.
36. **Lokk K, Modhukur V, Rajashekar B, Märtens K, Mägi R, Kolde R, Koltšina M, Nilsson TK, Vilo J, Salumets A, Tõnisson N.** DNA methylome profiling of human tissues identifies global and tissue-specific methylation patterns. *Genome Biol* 15: r54, 2014. doi:10.1186/gb-2014-15-4-r54.
37. **Lomax RG, Hahs-Vaughn DL.** *Statistical Concepts: A Second Course*. New York: Routledge Chapman & Hall, 2012.
38. **López-Otín C, Blasco MA, Partridge L, Serrano M, Kroemer G.** The hallmarks of aging. *Cell* 153: 1194–1217, 2013. doi:10.1016/j.cell.2013.05.039.
39. **Love MI, Huber W, Anders S.** Moderated estimation of fold change and dispersion for RNA-seq data with DESeq2. *Genome Biol* 15: 550, 2014. doi:10.1186/s13059-014-0550-8.
40. **Madrigano J, Baccarelli A, Mittleman MA, Sparrow D, Vokonas PS, Tarantini L, Schwartz J.** Aging and epigenetics: longitudinal changes in gene-specific DNA methylation. *Epigenetics* 7: 63–70, 2012. doi:10.4161/epi.7.1.18749.
41. **Manoharan H, Babcock K, Pitot HC.** Changes in the DNA methylation profile of the rat H19 gene upstream region during development and transgenic hepatocarcinogenesis and its role in the imprinted transcriptional regulation of the H19 gene. *Mol Carcinog* 41: 1–16, 2004. doi:10.1002/mc.20036.
42. **Mansell T, Novakovic B, Meyer B, Rzehak P, Vuillermin P, Ponsonby AL, Collier F, Burgner D, Saffery R, Ryan J, Vuillermin P, Ponsonby A-L, Carlin JB, Allen KJ, Tang ML, Saffery R, Ranganathan S, Burgner D, Dwyer T, Jachno K, Sly P; BIS investigator team.** The effects of maternal anxiety during pregnancy on IGF2/H19 methylation in cord blood. *Transl Psychiatry* 6: e765, 2016. doi:10.1038/tp.2016.32.
43. **McCarthy NS, Melton PE, Cadby G, Yazar S, Franchina M, Moses EK, Mackey DA, Hewitt AW.** Meta-analysis of human methylation data for evidence of sex-specific autosomal patterns. *BMC Genomics* 15: 981, 2014. doi:10.1186/1471-2164-15-981.
44. **McCormick JA, Lyons V, Jacobson MD, Noble J, Diorio J, Nyirenda M, Weaver S, Ester W, Yau JL, Meaney MJ, Seckl JR, Chapman KE.** 5′-Heterogeneity of glucocorticoid receptor messenger RNA is tissue specific: differential regulation of variant transcripts by early-life events. *Mol Endocrinol* 14: 506–517, 2000. doi:10.1210/mend.14.4.0438.
45. **Messerschmidt DM, Knowles BB, Solter D.** DNA methylation dynamics during epigenetic reprogramming in the germline and preimplantation embryos. *Genes Dev* 28: 812–828, 2014. doi:10.1101/gad.234294.113.
46. **Motulsky HJ, Ransnas LA.** Fitting curves to data using nonlinear regression: a practical and nonmathematical review. *FASEB J* 1: 365–374, 1987.
47. **Mueller BR, Bale TL.** Sex-specific programming of offspring emotionality after stress early in pregnancy. *J Neurosci* 28: 9055–9065, 2008. doi:10.1523/JNEUROSCI.1424-08.2008.
48. **Muller M, Renkawitz R.** The glucocorticoid receptor. *Biochim Biophys Acta* 1088: 171–182, 1991. doi:10.1016/0167-4781(91)90052-N.
49. **Ostlund BD, Conradt E, Crowell SE, Tyrka AR, Marsit CJ, Lester BM.** Prenatal stress, fearfulness, and the epigenome: exploratory analysis of sex differences in DNA methylation of the glucocorticoid receptor gene. *Front Behav Neurosci* 10: 147, 2016. doi:10.3389/fnbeh.2016.00147.
50. **Otto C, Stadler PF, Hoffmann S.** Fast and sensitive mapping of bisulfite-treated sequencing data. *Bioinformatics* 28: 1698–1704, 2012. doi:10.1093/bioinformatics/bts254.
51. **Palma-Gudiel H, Córdova-Palomera A, Leza JC, Fañanás L.** Glucocorticoid receptor gene (NR3C1) methylation processes as mediators of early adversity in stress-related disorders causality: A critical review. *Neurosci Biobehav Rev* 55: 520–535, 2015. doi:10.1016/j.neubiorev.2015.05.016.
52. **Perlman WR, Webster MJ, Herman MM, Kleinman JE, Weickert CS.** Age-related differences in glucocorticoid receptor mRNA levels in the human brain. *Neurobiol Aging* 28: 447–458, 2007. doi:10.1016/j.neurobiolaging.2006.01.010.
53. **Presul E, Schmidt S, Kofler R, Helmberg A.** Identification, tissue expression, and glucocorticoid responsiveness of alternative first exons of the human glucocorticoid receptor. *J Mol Endocrinol* 38: 79–90, 2007. doi:10.1677/jme.1.02183.
54. **R_Core_Team.** R: *A Language and Environment for Statistical Computing*. Vienna, Austria: R Foundation for Statistical Computing. https://www.R-project.org
55. **Ratajczak MZ.** Igf2-H19, an imprinted tandem gene, is an important regulator of embryonic development, a guardian of proliferation of adult pluripotent stem cells, a regulator of longevity, and a 'passkey' to cancerogenesis. *Folia Histochem Cytobiol* 50: 171–179, 2012. doi:10.5603/FHC.2012.0026.
56. **Rose AJ, Herzig S.** Metabolic control through glucocorticoid hormones: an update. *Mol Cell Endocrinol* 380: 65–78, 2013. doi:10.1016/j.mce.2013.03.007.
57. **Seckl JR.** Glucocorticoid programming of the fetus; adult phenotypes and molecular mechanisms. *Mol Cell Endocrinol* 185: 61–71, 2001. doi:10.1016/S0303-7207(01)00633-5.
58. **Sengupta P.** the laboratory rat: relating its age with human's. *Int J Prev Med* 4: 624–630, 2013.
59. **Smoak KA, Cidlowski JA.** Mechanisms of glucocorticoid receptor signaling during inflammation. *Mech Ageing Dev* 125: 697–706, 2004. doi:10.1016/j.mad.2004.06.010.
60. **Thorvaldsen JL, Duran KL, Bartolomei MS.** Deletion of the H19 differentially methylated domain results in loss of imprinted expression of H19 and Igf2. *Genes Dev* 12: 3693–3702, 1998. doi:10.1101/gad.12.23.3693.
61. **Turner JD, Alt SR, Cao L, Vernocchi S, Trifonova S, Battello N, Muller CP.** Transcriptional control of the glucocorticoid receptor: CpG islands, epigenetics and more. *Biochem Pharmacol* 80: 1860–1868, 2010. doi:10.1016/j.bcp.2010.06.037.
62. **Turner JD, Muller CP.** Structure of the glucocorticoid receptor (NR3C1) gene 5′ untranslated region: identification, and tissue distribution of multiple new human exon 1. *J Mol Endocrinol* 35: 283–292, 2005. doi:10.1677/jme.1.01822.
63. **Turner JD, Pelascini LP, Macedo JA, Muller CP.** Highly individual methylation patterns of alternative glucocorticoid receptor promoters suggest individualized epigenetic regulatory mechanisms. *Nucleic Acids Res* 36: 7207–7218, 2008. doi:10.1093/nar/gkn897.
64. **Weaver IC, Cervoni N, Champagne FA, D'Alessio AC, Sharma S, Seckl JR, Dymov S, Szyf M, Meaney MJ.** Epigenetic programming by maternal behavior. *Nat Neurosci* 7: 847–854, 2004. doi:10.1038/nn1276.
65. **Wilson VL, Jones PA.** DNA methylation decreases in aging but not in immortal cells. *Science* 220: 1055–1057, 1983. doi:10.1126/science.6844925.
66. **Yang X, Shao X, Gao L, Zhang S.** Systematic DNA methylation analysis of multiple cell lines reveals common and specific patterns within and across tissues of origin. *Hum Mol Genet* 24: 4374–4384, 2015. doi:10.1093/hmg/ddv172.
67. **Zhao L, Sun MA, Li Z, Bai X, Yu M, Wang M, Liang L, Shao X, Arnovitz S, Wang Q, He C, Lu X, Chen J, Xie H.** The dynamics of DNA methylation fidelity during mouse embryonic stem cell self-renewal and differentiation. *Genome Res* 24: 1296–1307, 2014. doi:10.1101/gr.163147.113.